ISSN 1062-8738, Bulletin of the Russian Academy of Sciences: Physics, 2022, Vol. 86, No. 5, pp. 610–613. © Allerton Press, Inc., 2022.
Russian Text © The Author(s), 2022, published in Izvestiya Rossiiskoi Akademii Nauk, Seriya Fizicheskaya, 2022, Vol. 86, No. 5, pp. 726–729.

Synthesizing Antiferromagnetic α-Fe_2O_3–rGO Discs: Their Magnetic and Magneto-Optical Properties

A. V. Kurilova[a], *, A. E. Sokolov[b], A. L. Sukhachev[b], O. S. Ivanova[b], K. V. Bogdanov[a], M. A. Baranov[a], and A. Yu. Dubavik[a]

[a] *ITMO National Research University, St. Petersburg, 197101, Russia*

[b] *Kirensky Institute of Physics, Siberian Branch, Russian Academy of Sciences, Krasnoyarsk, 660036 Russia*

**e-mail: list.ru-00@inbox.ru*

Received December 13, 2021; revised December 24, 2021; accepted January 21, 2022

Abstract—A comprehensive study is performed of the properties of hybrid structures of iron oxide and reduced graphene oxide α-Fe_2O_3/rGO synthesized via "wet mixing." It is shown that hematite nanoparticles with a comparatively uniform distribution can be encapsulated in graphene layers, and the way of preparing precursors is of critical importance in shaping the magneto-optical properties of α-Fe_2O_3/rGO hybrid structures.

DOI: 10.3103/S106287382205015X

INTRODUCTION

Along with a large surface area, graphene—a hexagonal 2D crystal lattice of a carbon atom monolayer with sp^2-hybrid orbitals connected by σ- and π-bonds—exhibits unique electric and thermal conductivity, plasticity, and chemical stability, providing persistent scientific interest in it and drives the search for different applications [1, 2]. Studies published in the early 2000s showed that graphene can also have magnetic properties [3–5]. In the opinion of most researchers, the material can exhibit ferromagnetic ordering as a result of, e.g., the chemisorption of hydrogen or induced defects of magnetic moments bound by ferromagnetic interaction [5]. It should be noted that the processes generated by defects are very weak and unpredictable, so graphene can exhibit superparamagnetic, paramagnetic, and antiferromagnetic properties in addition to ferromagnetism. It was reported in [6] that hydroxyl function groups on a surface of graphene oxide can induce a paramagnetic state. An option for enhancing magnetic properties is to combine a graphene/graphenelike structure with other materials [7] or use it as a functional matrix [8].

The familiar magnetic superconductor α-Fe_2O_3—the final product of the thermal transformation of different Fe^{2+} and Fe^{3+} compounds and the most thermally stable iron oxide polymorph—in turn has many potential applications in, e.g., medicine [9], electromagnetic-wave absorbers [10], information storage systems, and highly efficient photocatalysts [11, 12]. A combination of reduced graphene oxide (rGO) and nanoparticles of iron oxide α-Fe_2O_3 alters the magnetic, optical, and magneto-optical properties of the system. Although Fe^{3+} ion spins are reoriented toward trigonal axis [111] below the Morin point (T_M for hematite is 250–260 K) and the crystal becomes a pure antiferromagnetic, this does not prevent the use of α-Fe_2O_3/rGO composites as gas sensors [13], electrochemical sensors [14], water purification filters, photocatalysts [15], cathode material for lithium-ion batteries [4], anode material for sodium-ion batteries [16], and other purposes [17].

The aim of this work was to study the optical and magneto-optical properties of α-Fe_2O_3/rGO nanostructures and the magnetic properties of composite components and complete systems. Absorption spectroscopy, Raman scattering, magnetic circular dichroism, and scanning electron microscopy were used to analyze these properties.

EXPERIMENTAL

Preparing Hexagonal α-Fe_2O_3 Plates

The synthesis of hexagonal α-Fe_2O_3 plates was described in detail in [18]. Powder of $FeCl_3 \cdot 6H_2O$ (0.28 g) and sodium acetate (0.79 g) was dissolved in ethanol (10.0 mL) and water (0.7 mL) with intense mixing on a magnetic mixer. After the color of the solution became red, the mixture was sealed for 12 h in an airtight autoclave made of Teflon-coated stainless steel at 180°C. At the end of this period, the sample was allowed to cool to room temperature and washed several times with distilled water and ethanol.

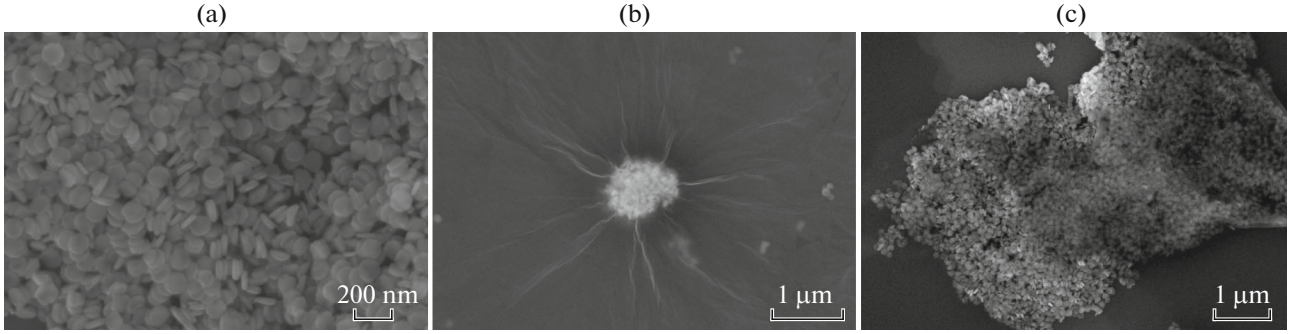

Fig. 1. SEM images of (a) α-Fe_2O_3 nanodiscs, (b) α-Fe_2O_3–rGO composite material (sample 1), and (c) α-Fe_2O_3–rGO composite material (sample 2).

Preparing the α-Fe_2O_3–rGO Hybrid Structure

Our α-Fe_2O_3–rGO hybrid structure was synthesized via wet mixing [19]. To synthesize sample 1, we used a pre-dissolved in poly(sodium 4-styrenesulfonate) powder of reduced graphene oxide (Aldrich, Germany) at a concentration of 10 mg/mL and a 1 : 1 mass ratio with iron oxide nanoplates. Forty milligrams of α-Fe_2O_3 nanoplates dissolved in 10 mL of ethanol were mixed intensely with 4 mL of rGO for 3 h at 60°C.

In synthesizing sample 2, we changed the volume of the solvent and the way of preparing the precursor. A mixture of 20 mg of α-Fe_2O_3 nanoplates dissolved in 1 mL of ethanol and 20 mg of rGO powder (Aldrich, Germany) were mixed intensely for 3 h at 60°C. The samples were allowed to cool to room temperature, washed several times with water, and stored in ethanol at room temperature.

Characterizing Samples

A Merlin scanning electron microscope (SEM) (Zeiss, Oberkochen, Germany) was used to visualize the dimensions and shapes of our samples. Optical absorption spectra in the spectral range of 300–800 nm were measured using a Shimadzu UV3600 spectrophotometer. Spectral dependences of magnetic circular dichroism (MCD) were measured by modulating light beam polarization in the 450–1000 nm range. The angle of rotation was measured with an accuracy of ±0.2 min. MCD was measured with an accuracy of $\pm 10^{-5}$. The external magnetic field was oriented along the light beam, normal to the sample surface. The accuracy of field measurements was ±20 Oe.

RESULTS AND DISCUSSION

The obtained α-Fe_2O_3 hexagonal plates were nanoparticles ~26 nm thick, with an average size of 107 nm and a narrow size distribution (Fig. 1a). Figures 1b, 1c show the graphene coating obtained in synthesizing α-Fe_2O_3–rGO hybrid structures was nonuniform (zonal). It was difficult to determine the thickness of the coating in this manner, but semitransparent graphene sheets were in both cases clearly distinguished. Sample 1 had a true core–shell structure, in which several hundred hematite nanoparticles serve as the core (Fig. 1b).

The presence of graphene oxide in our samples was confirmed by the D and G peaks in Raman scattering spectra, which are typical of carbon structures (Fig. 2a). The intense D peak near 1345–1360 cm^{-1} was due to the whispering mode of carbon atoms in defective C6 rings, while the G-peak in the vicinity of 1580–1610 cm^{-1} was associated with the extension of the sp^2 bond of carbon pairs. The intense 2D peak exhibited by the samples at 2665–2720 cm^{-1} corresponded to a D-peak overtone [20, 21]. Transitions characteristic of hematite (223, 244, 293, 407, 612, and 1324 cm^{-1}) were also discovered. The signal at 656 cm^{-1} indicated the samples contained amounts of wustite FeO. The clearly pronounced peaks at 973 and 1628 cm^{-1} were caused by solvents. The two spectra for sample 2 in Fig. 2a testify to the nonuniformity of the graphene oxide on the nanoplates, indicating there were areas with a negligible signal from graphene (i.e., graphene could be present at one point and missing at another).

Figure 2b presents optical absorption spectra. We can see that the α-Fe_2O_3 nanoplates had absorption bands characteristic of this phase, and the shape of the spectrum coincides with that of the coefficient of absorption of the α-Fe_2O_3 single crystal given in [22]. In contrast to the original core, the absorption spectra of samples 1 and 2 kept exhibiting a rise of absorption in the shortwave part of the spectrum, due most likely to graphene oxide contributing to a loss of transparency. The presence of graphene led to additional bands not observed in original discs emerging in the vicinity of 1.9 eV (sample 1) and 1.6 eV (sample 2).

Figure 3 presents the MCD spectrum of original α-Fe_2O_3 plates and samples 1 and 2 at room tempera-

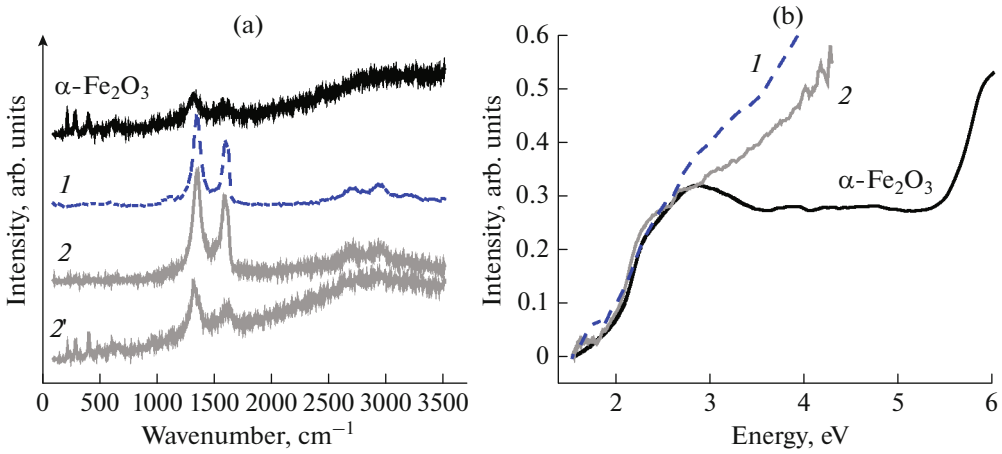

Fig. 2. Optical spectra of (a) the Raman spectra and (b) absorption of α-Fe_2O_3 nanodiscs for samples 1 (curves *1*) and 2 (curves *2* and *2'*).

ture. The spectrum of the α-Fe_2O_3 nanoplates is similar to those observed for, e.g., α-Fe_2O_3 nanoparticles [22] and the equatorial Kerr effect of massive α-Fe_2O_3 in reflections from plane [111] [23]. This confirms the nanoplates contained hematite of the pure iron oxide phase. A characteristic feature of hematite in the MCD spectra is the S-shaped transition at 2.1–2.5 eV. It should be noted that although the MCD spectrum of hematite is recognizable, the association between specific features and certain electron transitions is not unique. Interpreting the spectra is a challenging problem, and researchers use a variety of ways to solve it [22, 24–26]. Due to overlapping contributions from multiple transitions, the interpretation of iron oxide spectra is not unique.

Since MCD is observed in a region of absorption and does not normally contain a contribution from the nonmagnetic medium component, changes in the MCD spectrum can be used to track different changes in the magnetic state. The shapes of the MCD spectra of hematite and sample 1 (Fig. 3) are virtually the same; the magnitude of the signal is greatly diminished, and a negligible redistribution of band intensities is observed. However, the spectrum of sample 2 differs from the first two cases because it shows the strong effect graphene has on the magnetic state and thus electron transitions. Certain types of transitions are conventionally associated with specific energy ranges, and the substantial changes in the MCD spectrum of sample 2 testifies to the strong effect graphene oxide has on charge-transfer transitions (3.1–4.96 eV) and pairwise excitations (2.07–3.1 eV), along with its negligible influence on weaker transitions as a result of splitting in the crystalline field (1.39–2.07 eV).

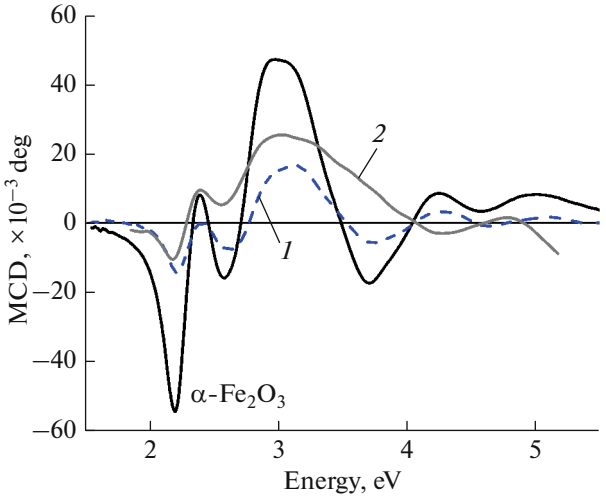

Fig. 3. MCD spectra of α-Fe_2O_3 nanodiscs at room temperature, measured in a field of 1.5 T.

CONCLUSIONS

We studied the structural, optical, and magneto-optical properties of α-Fe_2O_3/rGO hybrid structures synthesized via wet mixing. It was found that hematite nanoparticles with a relatively uniform size distribution can be encapsulated in graphene layers. At the same time, the method of preparation of the precursor during synthesis plays a key role both on the formation of the "habitat" of α-Fe_2O_3 nanodiscs and on the magneto-optical properties of hybrid α-Fe_2O_3/rGO structures.

REFERENCES

1. Glazov, S.Yu., *Bull. Russ. Acad. Sci.: Phys.*, 2019, vol. 83, no. 1, p. 12.
2. Shesterikov, A.V. and Prokhorov, A.V., *Bull. Russ. Acad. Sci.: Phys.*, 2020, vol. 84, no. 3, p. 319.
3. Yazyev, O.V., *Rep. Prog. Phys.*, 2010, vol. 73, no. 5, 056501.

4. Chen, D., Quan, H., Liang, J., and Guo, L., *Nanoscale*, 2013, vol. 5, no. 20, p. 9684.
5. Sarkar, S.K., Raul, K.K., Pradhan, S.S., et al., *Phys. E (Amsterdam, Neth.)*, 2014, vol. 64, p. 78.
6. Kim, S.-W., Kim, H.-K., Lee, K., et al., *Carbon*, 2019, vol. 142, p. 373.
7. Kochervinskii, V.V., *Bull. Russ. Acad. Sci.: Phys.*, 2020, vol. 84, no. 2, p. 144.
8. Rajaura, R.S., Sharma, V., Ronin, R.S., et al., *Mater. Res. Exp.*, 2017, vol. 4, no. 2, 025401.
9. Lunin, A.V., Lizunova, A.A., Mochalova, E.N., et al., *Molecules*, 2020, vol. 25, no. 8, p. 1984.
10. Guo, C.Y., Xia, F.Y., Wang, Z., et al., *J. Alloys Compd.*, 2015, vol. 631, p. 183.
11. Sharma, P., Dhiman, S., Kumari, S., et al., *Mater. Res. Exp.*, 2019, vol. 6, no. 9, 095072.
12. Panikar, A.S., Pan, S.L., and Gupta, A., *Abstr. Pap. Am. Chem. Soc.*, 2013, vol. 245.
13. Guo, L.L., Kou, X.Y., Ding, M.D., et al., *Sens. Actuators, B*, 2017, vol. 244, p. 233.
14. Mathew, G., Dey, P., and Das, R., et al., *Biosens. Bioelectron.*, 2018, vol. 115, p. 53.
15. Satheesh, M., Paloly, A.R., Sagar, C.K., et al., *Phys. Status Solidi A*, 2018, vol. 215, no. 2, 1700705.
16. Modafferi, V., Triolo, C., Fiore, M., et al., *Nanomaterials*, 2020, vol. 10, no. 8, p. 1588.
17. Lawal, A.T., *Biosens. Bioelectron.*, 2019, vol. 141, 111384.
18. Chen, L., Yang, X.F., Chen, J.A., et al., *Inorg. Chem.*, 2010, vol. 49, no. 18, p. 8411.
19. Mufida, R.Y. and Kusumawati, D.H., *J. Phys.: Conf. Ser.*, 2020, vol. 1491, 012059.
20. Lyubutin, I.S., Baskakov, A.O., Starchikov, S.S., et al., *Mater. Chem. Phys.*, 2018, vol. 219, p. 411.
21. Klimenko, I.V., Lobanov, A.V., Trusova, E.A., and Schegolikhin, A.N., *Russ. J. Phys. Chem. B*, 2019, vol. 13, p. 964.
22. Ivantsov, R., Ivanova, O., Zharkov, S., et al., *J. Magn. Magn. Mater.*, 2020, vol. 498, 166208.
23. Krinchik, G.S., Khrebtov, A.P., Askochenskii, A.A., and Zubov, V.E., *Zh. Eksp. Teor. Fiz.*, 1973, vol. 17, no. 9, p. 466.
24. Fontijn, W.F.J., Zaag, P.J., Feiner, L.F., et al., *J. Appl. Phys.*, 1999, vol. 85, p. 5100.
25. Piccinin, S., *Phys. Chem. Chem. Phys.*, 2019, vol. 21, p. 2957.
26. Pisarev, R.V., Moskvin, A.S., Kalashnikova, A.M., and Rasing, Th., *Phys. Rev. B*, 2009, vol. 79, 235138.

Translated by M. Shmatikov